PCCP

Cite this: *Phys. Chem. Chem. Phys.*, 2012, **14**, 367–374

www.rsc.org/pccp

PAPER

Activation of C–Cl by ground-state aluminum atoms: an EPR and DFT investigation

Helen A. Joly,* Trevor Newton† and Maxine Myre

Received 24th July 2011, Accepted 28th October 2011
DOI: 10.1039/c1cp22398d

The reaction of ground-state Al atoms with dichloromethane (CH_2Cl_2) in an adamantane matrix at 77 K yielded two mononuclear Al species. The magnetic parameters, extracted from the axial EPR spectrum of Species A/A′ (g_1 = 2.0037, $g_2 = g_3$ = 2.0030, $a_{Al,1}$ = 1307 MHz, $a_{Al,2} = a_{Al,3}$ = 1273 MHz, a_{35Cl} = 34 MHz and a_{37Cl} = 28 MHz) were assigned to the Al-atom insertion product, $ClCH_2AlCl$. Density functional theory (DFT) calculations of the values of the Al and Cl hyperfine interaction (hfi) of the Cl_1–Cl_2 *gauche* conformer were in close agreement with the experimental values of $ClCH_2AlCl$. The second species, B/B′, had identical magnetic parameters to those of $ClCH_2AlCl$ with the exception that the Al hfi was 15% smaller. Coordination of a ligand, possessing a lone pair of electrons, to the Al atom of the insertion product, [$ClCH_2AlCl$]:X, could cause the a_{Al} to decrease by 15%. Alternatively, it is possible that the Cl_1–Cl_2 anti conformer of $ClCH_2AlCl$ is also isolated in the matrix. Support for the spectral assignments is given by calculation of the nuclear hfi of [$ClCH_2AlCl$]:H_2O and the Cl_1–Cl_2 anti conformer of $ClCH_2AlCl$ using a DFT method. The potential energy hypersurface for an Al atom approaching CH_2Cl_2, calculated at the B3LYP level, suggests that Al atom abstraction of Cl forming AlCl and CH_2Cl is favoured in the gas phase. When produced in a matrix, the close proximity of AlCl and CH_2Cl could account for the formation of $ClCH_2AlCl$. EPR evidence was also found for the formation of the $CHCl_2$ radical.

Introduction

A strategy used to destroy man-made environmental pollutants, such as halogenated organic compounds, involves finding ways to activate the C–Cl or C–F bonds.[1,2] Ground-state Al ($^2P_{1/2}$) atoms have been shown to activate a number of different types of bonds resulting in the formation of insertion products. Experiments involving NH_3,[3,4] H_2O,[5] H_2S, H_2Se,[6] CH_3OCH_3,[7,8] and CH_4[9] yielded $HAlNH_2$, HAlOH, HAlSH, HAlSeH, CH_3AlOCH_3 and CH_3AlH, respectively, indicating that Al atoms can activate N–H, O–H, S–H, Se–H, C–O and C–H bonds. Al atoms have also been reported to activate the C–C bond of cyclohexanol,[10] 1-methylcyclohexanol[10] and diethyl ether.[8,11] With respect to halogenated compounds, co-condensation of Al atoms with HCl in an Ar matrix resulted in the formation of HAlCl[12,13] at low concentration while increasing the HCl concentration to ~8% yielded $AlCl_2$. Finally, reaction of ground-state Al atoms with bromocyclopropane (CpBr) in adamantane at 77 K gave the two C–Br insertion products $CpAl^{79}Br$ and $CpAl^{81}Br$ as well as the allyl radical.[14]

Department of Chemistry and Biochemistry, Laurentian University, Ramsey Lake Road, Sudbury, ON P3E 2C6, Canada.
E-mail: hjoly@laurentian.ca; Fax: 705-675-4844;
Tel: 705-675-1151 ext. 2333
† Present address: Gowlings, Ottawa, ON, K1P 1C3, Canada.

The above-mentioned Al-centered radicals were characterized by EPR spectroscopy. The magnitude of the isotropic Al hyperfine interactions (hfi) of the radicals is related to the nature of the ligands attached to Al, *i.e.*, the Al hfi increases as the electron-withdrawing ability of the ligands increase.

Matrix-isolation infrared spectroscopy was used to study the reaction of Group 13 metal atoms (M) with halomethanes (CH_3X).[15,16] In the case of CH_3Br, a weak CH_3Br-M complex[16] formed at low temperatures (<77 K) while higher temperatures favoured the formation of a "Grignard reagent", CH_3MBr, *via* the oxidative addition[15,16] of CH_3Br to the metal. Insertion into the C–Br bond is the preferred reaction because of the low first ionization potentials (IP) of the Group 13 metal atoms and the large Group 13 metal–Br bond energies.[16] In a recent study[17] involving laser–ablated Pd atoms, Cho *et al.* found that only insertion complexes, HCX_2PdX formed in reactions with halomethanes containing H.

In the present study, the EPR investigation of the paramagnetic products resulting from the reaction of dichloromethane (CH_2Cl_2) with Al atoms, under matrix-isolation conditions, confirmed that C–Cl activation was possible. The spectral features are attributed to the Al-atom C–Cl insertion product, $ClCH_2AlCl$. Annealing the sample to higher temperatures led to the detection of a product with spectral features similar to those of $ClCH_2AlCl$ with the exception of the

magnitude of the Al hfi. The species is either $ClCH_2AlCl$ in another conformation or $[ClCH_2AlCl]$:X where X is H_2O. A comparison of the experimental values of the Al and Cl hfi to those calculated for $ClCH_2AlCl$ using density functional theory (DFT) supports the spectral assignments. A map of the potential energy hypersurface corresponding to the approach of an Al atom to CH_2Cl_2 indicated that in the gas phase formation of AlCl is barrierless. The combination of AlCl with CH_2Cl gives the observed insertion product. Finally, $CHCl_2$ dominates the center of the spectrum.

Experimental section

Preparation of Al atom–CH_2Cl_2 reaction mixtures

The CH_2Cl_2, CD_2Cl_2 and adamantane were the purest available commercial products (Aldrich) and were used as received after being subjected to a number of freeze-thaw cycles on a vacuum line.

The method used to prepare the reaction mixture of ground-state Al atoms with CH_2Cl_2 or CD_2Cl_2, has been described in detail elsewhere.[18] Aluminum wire, (Alpha Products) in a tungsten basket (No. 12070, Ernest F. Fullam, Inc., Schenectady, NY) suspended between the electrodes of a furnace, was resistively heated to produce Al atoms. The Al atoms, CH_2Cl_2 or CD_2Cl_2 and adamantane were co-condensed on the surface of the rotating liquid nitrogen-filled drum situated in the metal-atom reactor. During the experiment (*ca.* 10 to 12 min) the reactor was maintained at $<10^{-5}$ Torr. A sample of the reaction mixture was scraped into a suprasil quartz tube and sealed under vacuum while maintaining a temperature of 77 K. EPR analysis was carried out between 77 and 298 K on a Varian E line spectrometer operating an X-band. A Varian gaussmeter and a Systron-Donner 6016 frequency counter were used in obtaining calibrated spectra. The magnetic parameters of the paramagnetic products were determined using the computer programs, ESRLSQ,[19] EPRNMR[20] or ISOPLOT.[19]

Computational methods

(i) Geometry and nuclear hyperfine interaction (hfi)

The Gaussian 09[21] suite of programs was used to calculate the values of the Al, H and ^{35}Cl hfi for $ClCH_2AlCl$. Full geometry optimization of $ClCH_2AlCl$ was carried out at the correlated *ab initio* (QCISD method) and density functional levels of theory (B3LYP and B3P86). In the QCISD method[22] the electron correlation was included through configuration interaction. The B3LYP[23] functional combines Becke's three parameter exchange functional[24] with Lee, Yang and Parr's[25] correlation functional which includes both local and non-local terms. B3P86 combines the exchange functional mentioned above with the non-local correlation introduced by Perdew.[26] The split valence 6-31G(df,p) basis set was used in the optimization of the insertion radical's geometry. In an exploratory investigation of the $ClCH_2AlCl$ radical the 6-31G(df,p) basis set gave values for the Al hfi that agreed more closely with the experimental values than the basis set most often used in these types of calculations, namely the 6-31G(d,p).[10,13] The radical was characterized using frequency analysis. The Al, H and ^{35}Cl nuclear hfi values were determined from single point calculations using the following methods: B3LYP/6-311+G(2df,p), BHandHLYP/6-311+G(2df,p), BHandHLYP[25,27,28]/6-311G(d,p), and mPWP86[26,29,30]/IGLO-III.[31]

(ii) Born–Oppenheimer potential energy surface

The Born–Oppenheimer potential energy surface for the lowest-energy doublet was calculated at the B3LYP level with a 6-31G(df,p) basis set by optimizing the geometry of the radical with fixed C–Cl_1 and C–Al distances. We chose to investigate the energy cross-section over the (C–Al, C–Cl_1) plane using geometries in which the dihedral angle defined by Cl_2, C, Al, and Cl_1 was approximately 90°. In calculations where no constraint was placed on the structures, the dihedral angle defined by Cl_2, C, Al, and Cl_1 for the most stable geometry was 91.1°. The B3LYP functional was used so that a comparison could be made with results previously reported for a similar system, namely, the reaction of Al atoms with CpBr.[14]

Results

EPR analysis of the products resulting from the reaction of Al atoms with CH_2Cl_2 revealed two overlapping sextets, labeled $^{35}A/^{37}A$ and $^{35}B/^{37}B$ (Fig. 1), in addition to a strong central feature (C). Five of the six transitions, characteristic of mononuclear Al ($I = 5/2$) radicals, are indicated for both $^{35}A/^{37}A$ and $^{35}B/^{37}B$ on the EPR spectrum recorded at 145 K. Close inspection of the Al transitions for each of $^{35}A/^{37}A$ and $^{35}B/^{37}B$ revealed superhfi consistent with the unpaired electron interacting with a nucleus with $I = 3/2$. Chlorine has two EPR active isotopes ^{35}Cl ($I = 3/2$, $\mu = +0.82181\beta_n$, natural abundance = 75.53%)[32] and ^{37}Cl ($I = 3/2$, $\mu = +0.68407\ \beta_n$, natural abundance = 24.47%).[32] The high and low field features were simulated by assuming a mixture of $^{35}A/^{37}A$, with the magnetic parameters $g_1 = 2.0037 \pm 0.0003$, $g_2 = g_3 = 2.0030 \pm 0.0003$, a_1(Al) = 1307 ± 1 MHz, a_2(Al) = a_3 (Al) = 1273 ± 1 MHz, a_{35Cl} = 34 ± 1 MHz and a_{37Cl} = 28 ± 1 MHz and $^{35}B/^{37}B$ with the magnetic parameters $g_1 = g_2 = g_3 = 2.0030 \pm 0.0003$, a_1 (Al) = a_2(Al) = a_3 (Al) = 1086 ± 1 MHz,

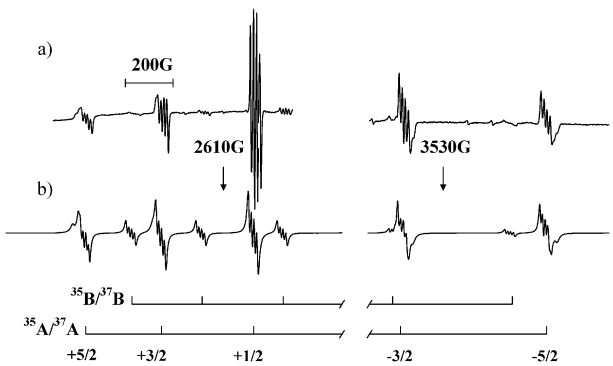

Fig. 1 (a) Five of the six Al EPR transitions for the paramagnetic species ($^{35}A/^{37}A$ and $^{35}B/^{37}B$) formed in the reaction of Al atoms with CH_2Cl_2 in an adamantane matrix. The low- and high-field regions of the EPR spectrum were recorded at 145 K (9120 MHz, microwave power [m.p. = 2 mW]); (b) Simulation of the low- and high-field regions of the EPR spectrum assuming the magnetic parameters for Species $^{35}A/^{37}A$ and for Species $^{35}B/^{37}B$ found in the text.

$a_{35Cl} = 34 \pm 1$ MHz and $a_{37Cl} = 28 \pm 1$ MHz. The $a_{35Cl}/a_{37Cl} = \mu_{35Cl}/\mu_{37Cl} = 1.21$ and the value of the $^{35}A/^{37}A$ and $^{35}B/^{37}B$ ratios used in the simulation was 3.09, *i.e.*, the ratio of the natural abundance of ^{35}Cl to ^{37}Cl. The best simulation was obtained using a ratio of ^{35}A to ^{35}B of 13 to 1.

The EPR spectrum of the major product, Species C, recorded at 195 K, shown in Fig. 2, was simulated using the magnetic parameters $g = 2.011$, $a_H(1) = 47.6$ MHz and $a_{Cl}(2) = 11.2$ MHz.

Mononuclear Al radicals with magnetic parameters similar to those of Species $^{35}A/^{37}A$ and $^{35}B/^{37}B$ were found for the reaction of Al atoms with CD_2Cl_2. A comparison of the Al transitions of $^{35}A/^{37}A$, Fig. 3a, and $^{35}B/^{37}B$, Fig. 3c, with those obtained in the Al atom–CD_2Cl_2 reaction (Fig. 3b and d) did not show noticeable narrowing indicating that the unpaired electron on Al does not interact with H atoms in the CH_2Cl_2. The EPR spectrum of the central feature of the Al atom–CD_2Cl_2 reaction was simulated with the magnetic parameters $g = 2.008$, $a_D(1) = 7.3$ MHz and $a_{Cl}(2) = 11.2$ MHz, Fig. 4. It should be noted that the a_D was estimated by dividing the value of a_H by 6.5, *i.e.*, the ratio of the magnetogyric ratios for the H and D nuclei.[32]

Computational results

We have been able to determine two stationary points for $ClCH_2AlCl$, namely, the Cl_1–Cl_2 *gauche* and Cl_1–Cl_2 anti conformers. The geometry of these conformers was optimized using three different levels of theory, Table 1. The DFT calculations indicate that the Cl_1–Cl_2 *gauche* conformer is slightly more stable than the anti conformer in the case of the B3LYP (0.7 kcal/mole) and the B3P86 (1.1 kcal/mole) calculations while the Cl_1–Cl_2 anti conformer is more stable in the QCISD calculations (0.8 kcal/mole). These small energy differences suggest that both of the two conformers are equally probable.

Single point calculations, using the computational methods listed in column 1 of Table 2 were used to determine the nuclear hfis of the *gauche* and anti conformers of $ClCH_2AlCl$. In the case of the Cl_1–Cl_2 *gauche* conformer the variation in the Al and Cl hfi is ≈6–7% and ≈10–12%, respectively, for all four methods tested. Similarly, the variation in the Al and Cl hfi is ≈2–3% and ≈9–10%, respectively, for the Cl_1–Cl_2 anti conformer. This indicates that the effect on the value of the Al hfi of using different levels of theory to optimize the geometry of the conformers is relatively small. In comparing the results for the two conformers optimized at the same level of theory we note that the Al and Cl hfi are larger for the Cl_1–Cl_2 *gauche* conformer in all cases. The increase in the value of the Al hfi in going from the anti to the *gauche* conformer is between 12–14%, 4–6% and 9–11% for the geometries optimized using the QCISD, B3LYP and B3P86 levels of theory, respectively, while the value of the Cl hfi increases by 8–13%, 7–12% and 8–14%, respectively. Although the variation in the H hfi is large for both conformers, it is interesting to note that (a) the hfi for H_1 and H_2 are approximately the same for the anti conformer while for the *gauche* conformer the H_1 hfi is larger than that of H_2; (b) the H_1 hfi of the anti conformer (1.3–5.6 MHz) is significantly smaller than that of the *gauche* conformer (10.5–16.1 MHz).

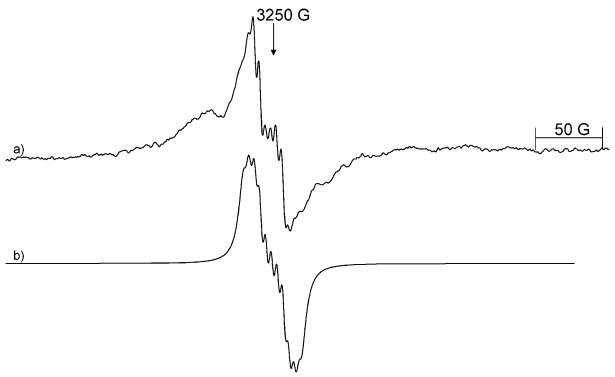

Fig. 2 (a) The central region of the EPR spectrum of the Al–CH_2Cl_2 reaction mixture recorded at 195 K (9120 MHz, m.p. = 20 mW). (b) Simulation of the central feature assuming $g = 2.011$, $a_H(1) = 47.6$ MHz, and $a_{Cl}(2) = 11.2$ MHz.

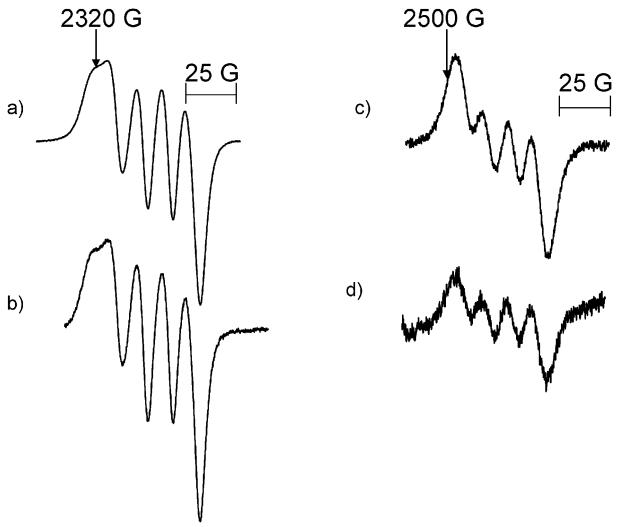

Fig. 3 The $M_I = 1/2$ transition of species $^{35}A/^{37}A$ formed in (a) the reaction of Al atoms with CH_2Cl_2 ($T = 115$ K, m.p. = 20 mW and $\nu = 9120$ MHz) (b) the reaction of Al atoms with CD_2Cl_2 ($T = 115$ K, m.p. = 20 mW and $\nu = 9121$ MHz). The $M_I = 1/2$ transition of species $^{35}B/^{37}B$ formed in (c) the reaction of Al atoms with CH_2Cl_2 ($T = 115$ K, m.p. = 20 mW and $\nu = 9120$ MHz) (d) the reaction of Al atoms with CD_2Cl_2 ($T = 115$ K, m.p. = 20 mW and $\nu = 9120$ MHz).

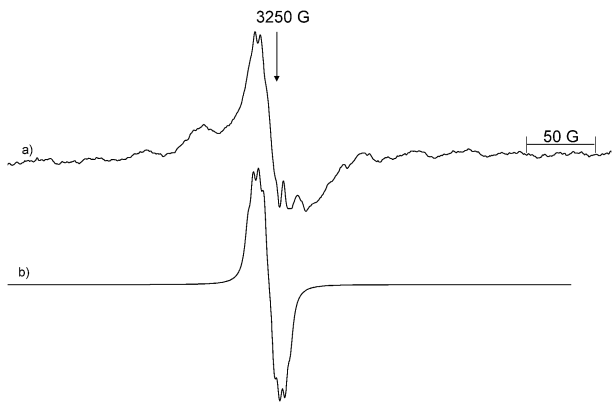

Fig. 4 (a) The central region of the EPR spectrum of the Al- CD_2Cl_2 reaction mixture recorded at 195 K (9119 MHz, m.p. = 20 mW). (b) Simulation of the central feature assuming $g = 2.008$, $a_D(1) = 7.3$ MHz and $a_{Cl}(2) = 11.2$ MHz.

Table 1 Optimized geometries corresponding to the Cl_1–Cl_2 *gauche* and anti conformers of $ClCH_2AlCl$. The interatomic distances, angles, dihedral angles and energy (hartrees) were obtained from QCISD/6-31G(df,p), B3LYP/6-31G(df,p), and B3P86/6-31G(df,p) calculations

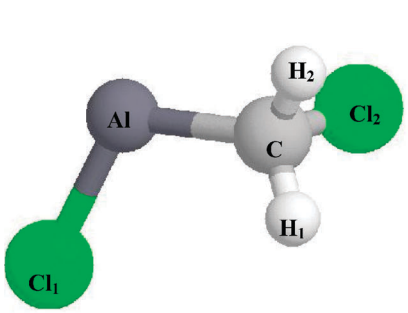

Cl_1-Cl_2 gauche

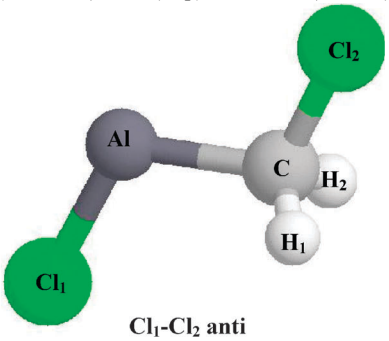

Cl_1-Cl_2 anti

	QCISD/6-31G(df,p)	B3LYP/6-31G(df,p)	B3P86/6-31G(df,p)	QCISD/6-31G(df,p)	B3LYP/6-31G(df,p)	B3P86/6-31G(df,p)
Cl_1–Al (Å)	2.099	2.134	2.124	2.098	2.139	2.126
Al–C (Å)	1.962	1.990	1.973	1.985	2.005	1.993
C–Cl_2 (Å)	1.845	1.847	1.844	1.788	1.815	1.799
C–H_1 (Å)	1.085	1.090	1.088	1.091	1.093	1.093
C–H_2 (Å)	1.086	1.089	1.089	1.091	1.093	1.093
∠$AlCCl_2$ (°)	82.4	94.3	87.0	111.2	111.5	110.7
∠$AlCH_1$ (°)	121.2	117.2	120.1	111.1	111.0	111.2
∠$AlCH_2$ (°)	121.1	118.0	119.5	111.1	111.0	111.2
∠Cl_1AlC (°)	117.7	116.9	116.7	115.9	114.2	114.5
D(Cl_2CAlCl_1) (°)	−93.0	−91.1	−91.9	180.0	180.0	180.0
D(H_2CAlCl_1) (°)	161.7	157.1	160.2	59.7	60.1	60.1
D(H_1CAlCl_1) (°)	12.5	20.8	16.2	−59.7	−60.1	−60.1
Energy (hartrees)	−1199.954657	−1202.177273	−1203.202415	−1199.955855	−1202.176135	−1203.200598

Table 2 The values of the Al, Cl and H hfi (in MHz) were calculated at the B3LYP/6-311+G(2df,p), BHandHLYP/6-311+G(2df,p), BHandHLYP/6-311G(d,p) and mPWP86/IGLO-III levels for the (a) Cl_1–Cl_2 *gauche* conformer and (b) Cl_1–Cl_2 anti conformer optimized at the QCISD/6-31G(df,p), B3LYP/6-31G(df,p) and B3P86/6-31G(df,p) levels of theory, respectively

		Geometry		
Method	Nuclei	QCISD/6-31G(df,p)	B3LYP/6-31G(df,p)	B3P86/6-31G(df,p)
(a) Cl_1–Cl_2 *gauche* conformation				
B3LYP/6-311+G(2df,p)	Al	1264.45	1182.53	1241.90
	Cl	37.42	33.30	34.66
	H_1, H_2	11.31, −5.80	14.43, −7.85	12.52, −6.76
BHandHLYP/6-311+G(2df,p)	Al	1298.68	1223.70	1280.22
	Cl	39.95	36.12	37.38
	H_1, H_2	10.51, −6.68	12.92, −9.22	11.43, −7.87
BHandHLYP/6-311G(d,p)	Al	1311.45	1234.80	1291.81
	Cl	39.45	35.64	36.84
	H_1, H_2	11.21, −6.61	13.55, −9.22	12.09, −7.84
mPWP86/IGLO-III	Al	1231.43	1145.07	1206.16
	Cl	34.15	30.22	31.53
	H_1, H_2	12.24, −4.80	16.10, −6.49	13.7, −5.59
(b) Cl_1–Cl_2 anti conformation				
B3LYP/6-311+G(2df,p)	Al	1099.25	1124.90	1117.31
	Cl	33.57	30.24	30.91
	H_1, H_2	3.11, 3.10	3.58, 3.58	3.31, 3.32
BHandHLYP/6-311+G(2df,p)	Al	1146.41	1177.04	1168.04
	Cl	36.94	33.70	34.38
	H_1, H_2	1.31, 1.30	1.58, 1.58	1.41, 1.42
BHandHLYP/6-311G(d,p)	Al	1155.39	1186.72	1177.11
	Cl	36.47	33.18	33.84
	H_1, H_2	1.32, 1.31	1.60, 1.60	1.43, 1.43
mPWP86/IGLO-III	Al	1059.09	1079.14	1073.69
	Cl	29.69	26.58	27.2
	H_1, H_2	4.92, 4.92	5.55, 5.54	5.18, 5.19

Discussion

Spectrum $^{35}A/^{37}A$

Spectrum $^{35}A/^{37}A$ can be described as two overlapping sextets of quartets corresponding to two mononuclear Al compounds containing ^{35}Cl and ^{37}Cl, respectively. The isotropic Al hfi, of $^{35}A/^{37}A$, calculated from the equation ($A_{iso} = (a_1 + a_2 + a_3)/3$),[32] is 1284 MHz. A comparison of this value to those reported in the literature for divalent Al radicals, Table 3, suggests that the C–Cl insertion products, $ClCH_2Al^{35}Cl$ and $ClCH_2Al^{37}Cl$

Table 3 The values of the nuclear hfi (in MHz) and Al 3s unpaired spin population (ρ_{3s}) of several mononuclear Al insertion products

Radical	a_{Al}	a_H	a_X	ρ_{3s}	Ref.
CH_3AlH	772	152	—	0.20	9
HAlH	834	128	—	0.21	33
HAlOH	911	286	—	0.23	5, 6
HOAlOH	1220	—	—	0.31	33
HAlSH	984	210	—	0.25	6
HAlSeH	941	134	20 (H)	0.24	6
HAlCl	1115	279	31 (Cl)	0.29	12, 13
ClAlCl	1598	—	31 (Cl)	0.41	12, 13
$ClCH_2AlCl$	1284	—	34 (Cl)	0.33	This work
$HAlNH_2$	923	229	27 (N) 27 (H)	0.24	3
CH_3AlOCH_3	1002	—	—	0.26	8
$CpAl^{79}Br$	1041	—	176 (^{79}Br)	0.27	14
$CpAl^{81}Br$	1042	—	190 (^{81}Br)	0.27	14

have generated Spectrum $^{35}A/^{37}A$. More specifically, the value of A_{iso} for $ClCH_2AlCl$ falls between that of HAlCl and ClAlCl. This is consistent with the observation[33] that the magnitude of the Al hfi increases as the electronegativity (or the electron-withdrawing ability) of the ligands increases. This is obvious in comparing the A_{iso} for HAlH, HAlCl and ClAlCl. Replacing H by Cl in going from HAlH to HAlCl causes the Al hfi to increase by 25% and by 30% in going from HAlCl to ClAlCl. As the ligands become more electron-withdrawing the ionic character of the σ-bonds to Al increases. This is translated to sp_x hybrid orbitals with greater p-character and a semi-occupied molecular orbital (SOMO) with higher s character. Therefore we would expect A_{iso} for $ClCH_2AlCl$ to be greater than that of HAlCl but less than that of ClAlCl because the electron-withdrawing ability of $ClCH_2$ is in between that of H and Cl.

The Al 3s-spin contribution, ρ_{3s}, to the SOMO, estimated by dividing the A_{iso} values for the divalent Al radicals by the one-electron atomic parameter for an Al 3s (3911 MHz)[32] orbital, has been included in Table 3. While the values range from 0.20–0.41, the ρ_{3s} for $ClCH_2AlCl$ is 0.33 indicating that the σ-bonds involving Al are slightly more ionic than those of HAlCl.

DFT methods have been very useful in predicting the Al hfi of a number of divalent organoaluminium radicals.[14,34,35] Many different density functionals are available. It is not obvious which are the best suited for use in the DFT calculation of nuclear hfi. One of the main factors influencing the selection of a functional is its reported effectiveness in predicting the nuclear hfi of well-characterized systems.[36] We have had success in predicting the Al hfi of several divalent Al compounds by optimizing their geometries with the split valence 6-31(d,p) basis set and determining the nuclear hfi with the B3LYP functional and the 6-311+G(2df,p) basis set.[35] This method predicted values that deviated from the experimental values by no more that 8%. In a theoretical study carried out by Fängström *et al.*[13] on the Al–atom insertion products of HCl and Cl_2, similar agreement was obtained between experiment and theory at the B3LYP/6-311+G(2df,p)//6-31G(d,p) and mPWP86/IGLO-III//QCISD/6-31G(d,p) levels. The Becke half and half functional (BHandH)[27,28] with the nonlocal correlation of Lee, Yang and Parr[25] (LYP) has been found to be effective in calculating the geometries and nuclear hfi of open shell systems.[37] Consequently, the nuclear hfi of the two conformers of $ClCH_2AlCl$ were calculated at the B3LYP/6-311+G(2df,p), BHandHLYP/6-311+G(2df,p), BHandHLYP/6-311G(d,p) and mPWP86/IGLO-III levels of theory, Table 2.

In general, the deviation between the experimental Al (1284 MHz) and ^{35}Cl (34 MHz) hfi and the calculated values is smaller for the *gauche* conformer; the Al and ^{35}Cl hfi deviate from the experimental values by 0.2–11% and 1–18%, respectively for the *gauche* conformer and by 8–17% and 1–22% for the anti conformer. The Al and ^{35}Cl hfi values calculated at the B3LYP/6-311+G(2df,p)//B3P86/6-31G(df,p) level of theory for the *gauche* isomer agree the best with the experimental values; *i.e.*, the deviation between the calculated and experimental values is 3% for the Al hfi and 2% for the Cl hfi. This is well within the expected error for these types of calculations.[14,34,35] At the same level of theory, the Al and Cl hfi calculated for the anti conformer differ from experiment by 13% and 9%, respectively. Experimentally the H hfi is too small to detect. The variation in the H hfi of the *gauche* conformer predicted by the different theoretical models is large making it difficult to draw any definitive conclusions.

Spectrum $^{35}B/^{37}B$

The spectral pattern labeled $^{35}B/^{37}B$ in Fig. 1 is identical to that of $^{35}A/^{37}A$, *i.e.*, a sextet of quartets. As in the case of $^{35}A/^{37}A$, one can deduce that the unpaired electron is interacting with an Al ($I = 5/2$) and a $^{35/37}Cl$ ($I = 3/2$) nucleus. The Al hfi (1086 MHz) extracted from the $^{35}B/^{37}B$ spectrum is 15% smaller than that of $ClCH_2AlCl$ while the ^{35}Cl and ^{37}Cl hfi are identical, *i.e.*, $a_{35Cl} = 34$ MHz and $a_{37Cl} = 28$ MHz.

As previously mentioned, the difference in the calculated energy for the Cl_1–Cl_2 *gauche versus* the anti conformer is small suggesting that both conformers are equally possible. In addition, the theoretical methods predict a decrease of up to 14% in the Al hfi in going from the *gauche* to the anti conformer. This is close to the 15% difference in Al hfi found between the Al hfi of Species $^{35}A/^{37}A$ and $^{35}B/^{37}B$. In a study involving the reaction of Al atoms with dimethyl ether, Kasai[7] found that both the *cis* and *trans* conformers of CH_3OAlCH_3 were formed. In this case the Al hfi for the *cis* conformer was greater than that for the *trans* conformer by 14%. Although theory predicted only a marginal difference in stability, the *trans* conformer was more abundant indicating that it was in fact more stable. $^{35}B/^{37}B$ could therefore be the Cl_1–Cl_2 anti conformer of $ClCH_2AlCl$. The fact that both the *gauche* and anti conformers are observed on the EPR time scale would suggest that the barrier for the interconversion of the two conformers is relatively high.

Alternately, a decrease in the Al hfi could be due to the coordination of the Al atom of $ClCH_2AlCl$ with a molecule containing a lone pair of electrons. For instance, in the reactions of Al atoms with NH_3 in Ar at 4 K,[4] cyclopropylamine in adamantane at 77 K,[35] and methoxymethane in Ar at 4 K[7] radicals producing identical spectral patterns differing only in the magnitude of the values of the nuclear hfi were detected. This phenomenon was attributed to complexation of a vacant coordination site of the divalent Al insertion products by a molecule containing a lone pair of electrons, Table 4. Coordination of NH_3 to $HAlNH_2$ results in the 18% decrease in the Al hfi.[4]

Table 4 Isotropic nuclear hfis (MHz) for the uncomplexed and complexed Al–atom insertion products as well as the % difference (Δ) in nuclear hfi

Nucleus	$HAlNH_2$[a]	$[HAlNH_2]:NH_3$[a]	%Δ in nuclear hfi
Al	950	779	−18%
H_1	213	95	−55%
H_2	27	28	+4%
N	27	28	+4%
	$CpNH(AlH)$[b]	$[CpNH(AlH)]:CpNH_2$[b]	%Δ in nuclear hfi
Al	962	801	−17%
H	216	133	−38%
N	32	23	−28%
	CH_3OAlCH_3[c]	$[CH_3OAlCH_3]:O(CH_3)_2$[c]	%Δ in nuclear hfi
Al	873	838	−4%
	$ClCH_2AlCl$[d]	$[ClCH_2AlCl]:X$[d]	%Δ in nuclear hfi
Al	1284	1086	−15%
^{35}Cl	34	34	0%

[a] Ref. 4. [b] Ref. 35. [c] Ref. 7. [d] This work.

The H hfi is estimated to decrease by 55% while the N hfi increases by about 4%. For $[CpNH(AlH)]:CpNH_2$, the Al, H and N hfi are 17, 38 and 28% smaller than that found for $CpNH(AlH)$.[35] Kasai suggested that the radical with an Al hfi that was 4% smaller than that of CH_3AlOCH_3 was the complexed insertion product $[CH_3AlOCH_3]:O(CH_3)_2$. This suggests that ^{35}B /^{37}B could be a mixture of $[ClCH_2Al^{35}Cl]:X$ and $[ClCH_2Al^{37}Cl]:X$ where X is a molecule with a lone pair of electrons. X could be H_2O from adventitious water present in the cryostat. This possibility was tested by carrying out an exploratory DFT calculation. The geometry of the $[ClCH_2AlCl]:OH_2$ complex was optimized using the B3LYP and B3P86 functionals and the 6-31G(df,p) basis set, Table 5. The Al and Cl hfi were obtained from a single point calculation using the B3LYP/6-311+G(2df,p), BHandHLYP/6-311+G(2df,p) and BHandHLYP/6-311G(d,p) levels of theory, Table 6. The Al hfi and Cl hfi for $[ClCH_2AlCl]:OH_2$ differed from those of the *gauche* conformation of $ClCH_2AlCl$ by 10–16% and 15–19%, respectively, at the same level of theory (Table 2 and 6). The calculation shows that complexation of a water molecule to the Al atom of $ClCH_2AlCl$ causes the Al hfi to decrease by approximately the same amount as that observed between ^{35}A/^{37}A and ^{35}B/^{37}B.

Spectrum C

The 8-lined spectrum, separated by 64 MHz, that dominates the central region at 77 K, disappears at temperatures >77 K leaving behind a doublet of septets with magnetic parameters, $g = 2.011$, $a_H = 47.6$ MHz and $a_{35Cl} = 11.2$ MHz, similar to those reported for $CHCl_2$ produced by exposing CH_2Cl_2 to ^{60}Co γ-rays, *i.e.*, $g = 2.007$, $a_H = 56$ MHz and $a_{35Cl} = 11$ MHz.[38] The difference in the a_H may be due to the fact the spectra were recorded under different conditions. In fact, in another study[39] involving the γ-radiolysis of CH_2Cl_2, slightly different magnetic parameters were obtained for $CHCl_2$, *i.e.*, $g = 2.013$, $a_H = 56$ MHz and $a_{35Cl} = 18$ MHz. The magnetic parameters are sensitive to the structure of the radical which can be distorted depending upon the nature of the matrix used in the experiment, *i.e.*, adamantane *vs.* CH_2Cl_2.

There is some suggestion that the formation of Al-atom insertion products is a multistep process. Interaction of the

Table 5 The interatomic distances, angles, dihedral angles, and energy (hartrees) for the Cl_1–Cl_2 *gauche* conformer of $[ClCH_2AlCl]:OH_2$ were optimized using B3LYP/6-31G(df,p), and B3P86/6-31G(df,p) levels of theory

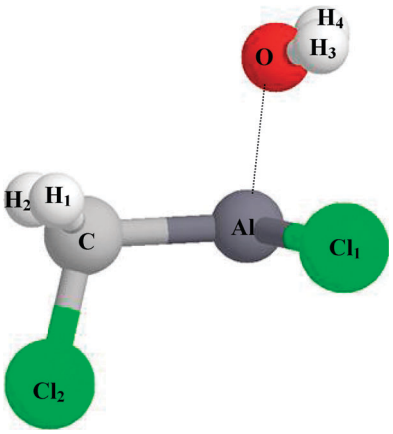

	B3LYP/6-31G(df,p)	B3P86/6-31G(df,p)
Cl_1–Al (Å)	2.185	2.174
Al–C (Å)	1.998	1.987
C–Cl_2 (Å)	1.831	1.814
C–H_1 (Å)	1.093	1.093
C–H_2 (Å)	1.092	1.092
O–Al (Å)	2.065	2.050
∠$AlCCl_2$ (°)	107.1	105.5
∠$AlCH_1$ (°)	113.7	114.1
∠$AlCH_2$ (°)	114.2	114.5
∠Cl_1AlC (°)	114.2	113.9
∠OAlC (°)	102.2	103.1
D(Cl_2CAlCl_1) (°)	84.0	83.9
D(Cl_2CAlO) (°)	−179.6	−179.3
D(H_2CAlCl_1) (°)	−158.6	−159.0
D(H_1CAlCl_1) (°)	−33.3	−33.1
Energy (hartrees)	−1278.630514	−1279.835873

Table 6 The values of the Al, Cl and H hfi (in MHz) were calculated at the B3LYP/6-311+G(2df,p), BHandHLYP/6-311+G(2df,p) and BHandHLYP/6-311G(d,p) levels for the Cl_1–Cl_2 *gauche* conformer of $[ClCH_2AlCl]:OH_2$ optimized at the B3LYP/6-31G(df,p) and B3P86/6-31G(df,p) levels of theory

		Geometry	
Method	Nuclei	B3LYP	B3P86
B3LYP/6-311+G(2df,p)	Al	1054.67	1044.43
	Cl	28.47	28.79
	H_1	17.30	16.88
	H_2	−5.90	−5.71
BHandHLYP/6-311+G(2df,p)	Al	1099.64	1087.93
	Cl	29.98	30.21
	H_1	16.21	15.89
	H_2	−6.70	−6.45
BHandHLYP/6-311G(d,p)	Al	1117.11	1104.95
	Cl	29.89	30.14
	H_1	17.19	16.87
	H_2	−6.81	−6.57

Al atoms with the substrate promotes bond cleavage and the resulting radicals recombine with the lone pair of electrons on the Al atom to form the insertion product. In the case of CH_3AlOCH_3, Kasai[7] proposed that Al atoms interact with a lone pair of electrons on the oxygen atom of dimethyl ether. Next, the C–O bond cleaves producing methyl radicals. The unpaired

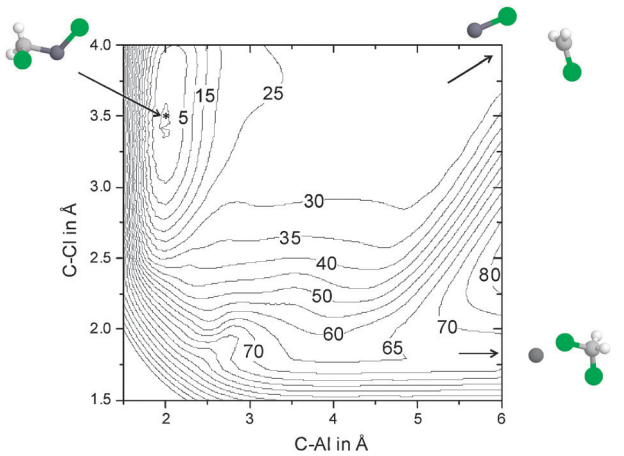

Fig. 5 Born–Oppenheimer potential energy surface of the lowest energy doublet for the reaction of Al atoms with CH_2Cl_2. The contour lines represent the energy in kcal/mole and are spaced by +5 kcal/mole. The minimum energy point was set to 0 kcal/mole and is denoted by *. The other minima (for AlCl + $ClCH_2$ and Al + CH_2Cl_2) are asymptotic and hence not indicated on the diagram.

electron of the methyl radical interacts with the lone pair electrons of the Al atom to form the insertion product, CH_3AlOCH_3.

As in the case of the Al atom activation of the C–Br bond in CpBr we decided to carry out a theoretical investigation of the mechanism of the Al–CH_2Cl_2 insertion reaction. The Al atom was made to approach the CH_2Cl_2 molecule. We chose to investigate the energy cross-section over the (C–Al, C–Cl_1) plane using geometries in which the dihedral angle defined by Cl_2, C, Al, and Cl_1 was approximately 90°. The geometry of structures with fixed Al–C and C–Cl_1 bond lengths were optimized at the B3LYP level with a 6-31G(d,p) basis set and a three dimensional plot of C–Al *versus* C–Cl_1 *versus* energy was constructed, Fig. 5. As in the case of the interaction of Al atoms and CpBr, the Al atom–CH_2Cl_2 reaction favours the formation of AlCl and CH_2Cl. There is no low energy channel that leads directly to the *gauche* conformer. The energy profile suggests that its formation is barrierless. Similarly the decomposition of $ClCH_2AlCl$ follows a barrierless channel that leads to AlCl and CH_2Cl. Presumably the recombination of AlCl and CH_2Cl trapped in an adamantane matrix could lead to the formation of the insertion product, $ClCH_2AlCl$.

We did not detect the CH_2Cl radical; however this may have something to do with its stability. In the study[39] involving the γ-radiolysis of CH_2Cl_2 at 77 K, the resulting EPR spectrum was attributed to a mixture of CH_2Cl and $CHCl_2$ in the ratio of 1 : 3. From this we could speculate that the CH_2Cl may have formed in our case but in concentrations too low to detect.

Conclusions

Two main radicals were detected in the Al–CH_2Cl_2 reaction, namely, $ClCH_2AlCl$ and $CHCl_2$. The large isotropic Al hfi for $ClCH_2AlCl$ falls between those reported for HAlCl and ClAlCl supporting the hypothesis that the Al hfi increases as the electron-withdrawing ability of the ligands increases. At higher annealing temperatures, a weak spectrum, identical to that of $ClCH_2AlCl$, with the exception of the Al hfi, was observed. The smaller Al hfi led us to attribute the spectrum to either the anti conformer of $ClCH_2AlCl$ or to $ClCH_2AlCl$:X where X possesses a lone pair of electrons, *e.g.*, as in the case of H_2O. The nuclear hfi calculated using a DFT method support the assignments. Exploration of a cross section of the potential energy surface for the Al–CH_2Cl_2 reaction shows that AlCl and CH_2Cl are favoured. The recombination of AlCl and CH_2Cl, trapped in an adamantane matrix, could lead to the formation of the insertion product, $ClCH_2AlCl$.

Acknowledgements

The Natural Sciences and Engineering Research Council of Canada (NSERCC) and Laurentian University are gratefully acknowledged for financial support. We would like to thank Ms Julie Feola and Mr Jean Pierre Rank for their technical assistance. We express our gratitude to Drs Gustavo Arteca, Sabine Montaut and Tony Howard for helpful discussions. The authors also wish to thank the reviewers for comments as they helped improve the paper.

References

1 C. L. Geiger, K. Carvalho-Knighton, S. Novaes-Card, P. Maloney and R. DeVor, in *Environmental Applications of Nanoscale and Microscale Reactive Metal Particles*, ACS Symp. Ser., 2009, vol. 1027, p. 1.
2 C. Douvris, C. M. Nagaraja, C.-H. Chen, B. M. Foxman and O. V. Ozerov, *J. Am. Chem. Soc.*, 2010, **132**, 4946.
3 J. A. Howard, H. A. Joly, P. P. Edwards, R. J. Singer and D. E. Logan, *J. Am. Chem. Soc.*, 1992, **114**, 474.
4 P. H. Kasai and H.-J. Himmel, *J. Phys. Chem. A*, 2002, **106**, 6765.
5 L. B. Knight, Jr., B. Gregory, J. Cleveland and C. A. Arrington, *Chem. Phys. Lett.*, 1993, **204**, 168.
6 H. A. Joly, J. A. Howard, M. Tomietto and J. S. Tse, *J. Chem. Soc., Faraday Trans.*, 1994, **90**, 3145.
7 P. H. Kasai, *J. Phys. Chem. A*, 2002, **106**, 83.
8 J. H. B. Chenier, J. A. Howard, H. A. Joly, M. LeDuc and B. Mile, *J. Chem. Soc., Faraday Trans.*, 1990, **86**, 3321.
9 J. M. Parnis and G. A. Ozin, *J. Phys. Chem.*, 1989, **93**, 1204.
10 H. A. Joly, J. A. Howard and G. A. Arteca, *Phys. Chem. Chem. Phys.*, 2001, **3**, 760.
11 J. A. Howard, H. A. Joly and B. Mile, *J. Chem. Soc., Faraday Trans.*, 1990, **86**, 219.
12 R. Köppe and P. H. Kasai, *J. Am. Chem. Soc.*, 1996, **118**, 135.
13 T. Fängström, S. Lunell, P. H. Kasai and L. A. Eriksson, *J. Phys. Chem. A*, 1998, **102**, 1005.
14 H. A. Joly, M. Y. Levesque, F. Koudra and J. P. Rank, *Chem. Phys. Lett.*, 2006, **420**, 140.
15 P. S. Skell and J. E. Girard, *J. Am. Chem. Soc.*, 1972, **94**, 5518.
16 B. S. Ault, *J. Am. Chem. Soc.*, 1980, **102**, 3480.
17 H.-G. Cho, L. Andrews, B. Vlaisavljevich and L. Gagliardi, *Organometallics*, 2009, **28**, 6871.
18 A. J. Buck, B. Mile and J. A. Howard, *J. Am. Chem. Soc.*, 1983, **105**, 3381.
19 K. F. Preston and J. R. Morton, *ISOPLOT and ESRLSQ*, National Research Council of Canada, Ottawa.
20 J. A. Weils, *EPR-NMR*, University of Saskatchewan, Saskatoon.
21 M. J. Frisch, G. W. Trucks, H. B. Schlegel, G. E. Scuseria, M. A. Robb, J. R. Cheeseman, G. Scalmani, V. Barone, B. Mennucci, G. A. Petersson, H. Nakatsuji, M. Caricato, X. Li, H. P. Hratchian, A. F. Izmaylov, J. Bloino, G. Zheng, J. L. Sonnenberg, M. Hada, M. Ehara, K. Toyota, R. Fukuda, J. Hasegawa, M. Ishida, T. Nakajima, Y. Honda, O. Kitao, H. Nakai, T. Vreven, J. A. Montgomery, Jr., J. E. Peralta, F. Ogliaro, M. Bearpark, J. J. Heyd, E. Brothers, K. N. Kudin, V. N. Staroverov, R. Kobayashi, J. Normand, K. Raghavachari, A. Rendell, J. C. Burant, S. S. Iyengar, J. Tomasi, M. Cossi, N. Rega, J. M. Millam, M. Klene, J. E. Knox, J. B. Cross, V. Bakken, C. Adamo, J. Jaramillo,

R. Gomperts, R. E. Stratmann, O. Yazyev, A. J. Austin, R. Cammi, C. Pomelli, J. Ochterski, R. L. Martin, K. Morokuma, V. G. Zakrzewski, G. A. Voth, P. Salvador, J. J. Dannenberg, S. Dapprich, A. D. Daniels, O. Farkas, J. B. Foresman, J. V. Ortiz, J. Cioslowski and D. J. Fox, *GAUSSIAN 09 (Revision A.1)*, Gaussian, Inc., Wallingford, CT, 2009.
22 J. A. Pople, M. Head-Gordon and K. Raghavachari, *J. Chem. Phys.*, 1987, **87**, 5968.
23 P. J. Stephens, F. J. Devlin, C. F. Chabalowski and M. J. Frisch, *J. Phys. Chem.*, 1994, **98**, 11623.
24 A. D. Becke, *J. Chem. Phys.*, 1993, **98**, 5648.
25 C. Lee, W. Yang and R. G. Parr, *Phys. Rev. B*, 1988, **37**, 785.
26 J. P. Perdew, *Phys. Rev. B*, 1986, **33**, 8822.
27 A. D. Becke, *Phys. Rev. A: At., Mol., Opt. Phys.*, 1988, **38**, 3098.
28 S. H. Vosko, L. Wilk and M. Nusair, *Can. J. Phys.*, 1980, **58**, 1200.
29 J. P. Perdew and W. Yue, *Phys. Rev. B*, 1986, **33**, 8800.
30 J. P. Perdew, *Phys. Rev. B*, 1986, **34**, 7406.
31 W. Kutzelnigg, U. Fleischer and M. Schindler, *NMR: Basic principles and Progress*, Springer-Verlag, 1990.
32 W. Weltner, Jr., *Magnetic Atoms and Molecules*, Dover, 1989.
33 L. B. Knight, Jr., J. R. Woodward, T. J. Kirk and C. A. Arrington, *J. Phys. Chem.*, 1993, **97**, 1304.
34 H. A. Joly, J. A. Howard and G. A. Arteca, *Phys. Chem. Chem. Phys.*, 2001, **3**, 750.
35 H. Joly, J. Ashley, M. Levesque and J. Rank, *J. Phys. Chem. A*, 2006, **110**, 3911.
36 H. M. Tuononen, T. Chivers, A. Armstrong, C. Fedorchuk and R. T. Boeré, *J. Organomet. Chem.*, 2007, **692**, 2705.
37 J.-F. Xiao, Z.-S. Li, Y.-H. Ding, J.-Y. Liu, X.-R. Huang and C.-C. Sun, *J. Phys. Chem. A*, 2001, **106**, 320.
38 S. P. Mishra, G. W. Neilson and M. C. R. Symons, *J. Chem. Soc., Faraday Trans. 2*, 1973, **69**, 1425.
39 S. Truszkowski and W. Szymański, *J. Radioanal. Nucl. Chem.*, 1994, **177**, 415.

